PERFORMANCE AND MAGNETIC MEASUREMENTS OF A FULL SCALE CROSS-SECTION MODEL OF A SUPERCONDUCTING 8° BENDING MAGNET SYSTEM

J. Allinger, G. Danby, B. DeVito, H. Foelsche, R. Gibbs, S. Hsieh,
J. Jackson, A. Prodell and A. Raag

Brookhaven National Laboratory
Upton, N.Y. 11973

Abstract

A 20-in. long, full-scale cross-section model of a superconducting 8° bending magnet has been constructed and tested at Brookhaven National Laboratory. A description of the model magnet and test assembly is given, and field measurements and magnet performance are discussed.

I. Model Magnet and Test Assembly

A superconducting 8° bending magnet system has been designed and is being assembled to deflect primary protons of momenta up to 30 GeV/c to the new North Experimental Area of the Brookhaven National Laboratory Alternating Gradient Synchrotron. To provide data on mechanical and thermal stability and verify computed field coordinates, a 20-in. long, full-scale cross-section model of the 8° magnets has been constructed, tested, and measured. The construction of the 20-in. model was also used to develop and evaluate fabrication and assembly techniques for the full-sized magnets.

The 20-in. model magnet is constructed around a 3.5-in. diameter pipe which constitutes the cold bore of the model but which will represent the inner wall of the annular magnet cryostat for the 8° magnets. The magnet is of a rectangular aperture "window-frame" type with the iron core surrounding a dipole coil package of rectangular cross section. The aperture in the iron is approximately 4 in. high by 6.25 in. wide. The magnet is 14.875 in. high and 17.125 in. wide overall. The basic circuit is illustrated in Fig. 1.

The coil construction for the model magnet utilizes insulating sheets of anodized high purity aluminum between each vertical layer of formvar-coated conductor. These aluminum sheets have been rolled to produce vertical grooves through which LHe circulates for enhanced heat transfer. These grooves terminate in horizontal LHe channels at the top and bottom of the coil package which are in contact with the iron. The very high thermal conductivity of the iron core and the very high thermal and electrical conductivity of the aluminum provide excellent thermal and dynamic stability.
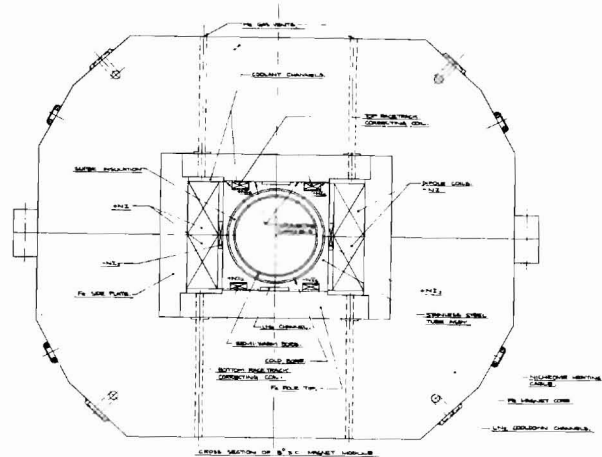
Fig. 1. Typical Cross-Section of the 20-in. Model for the 8° Superconducting Magnets.

The presence of the closely coupled iron surrounding the coil of the window-frame circuit reduces the ampere-turns required for magnetic fields below iron saturation by a factor between 2 and 3. Above saturation the ampere-turns required increases. The increase reaches 21 percent at 40 kG compared to infinite permeability. The systematic aberrations due to saturation at high fields are sufficiently large that an auxiliary correcting coil which is approximately an air-core sextupole is required for high optical precision. This coil must be excited increasingly as the field rises to 40 kG at which value it has an excitation of several percent of the main coil. This excitation, starting at about 20 kG, is essentially linear. With two separate excitation coils, which are uncoupled inductively, precision fields can be obtained at all levels.

The main dipole coils of the 20-in. model magnet are wound with 340 turns of formvar-coated composite conductor having an uninsulated cross section of 0.054 in. by 0.113 in. The conductor

has 1.25 to 1 copper to superconductor ratio and
contains 361 NbTi filaments, each approximately
3 mils in diameter, twisted one turn to the
inch.

TABLE I. 20-in. Model Magnet Parameters

Aperture, Diameter	3.375 in.
Magnetic Field Intensity	40 kG
Ampere-turns, Dipole Coil	408,000
Ampere-turns, Sextupole Coil	18,000
Current, Dipole Coil	1200 A
Current, Sextupole Coil	300 A
Current Density, Dipole Coil Conductor	3.05×10^4 A/cm^2
Current Density, Sextupole Coil Conductor	3.71×10^4 A/cm^2
Stored Energy	48 kJ
Inductance, Dipole Coil	55 mH

Details of the coil construction including
the magnet conductor and cooling channel sheets
are illustrated in Figs. 2 and 3. The cooling
channel sheets are of anodized aluminum along
the straight sections of the magnet coil and of
G-10 fiberglas epoxy around the ends.   Sections
of both the dipole and sextupole windings are
shown in Fig. 2 while only the dipole windings
are visible in Fig. 3. The completed model
magnet is shown in Fig. 4 with the harmonic
search coil probe used for field measurements
resting on top of the magnet.

Fig. 3.   End View of 20-in. Model Magnet Showing
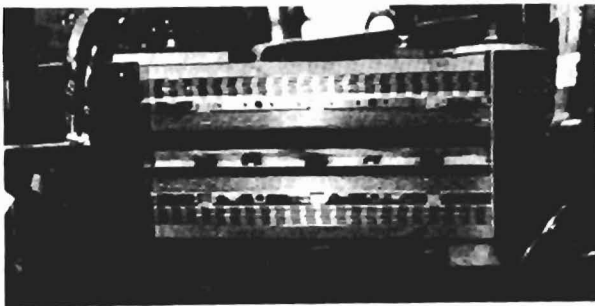the Dipole Windings and G-10 End Spacers.

Fig. 2.   Top View of the Straight Section of the
20-in. Model Magnet Showing the Dipole
Windings and Grooved Al Cooling Channel
Sheets Outside and the Finer Sextupole
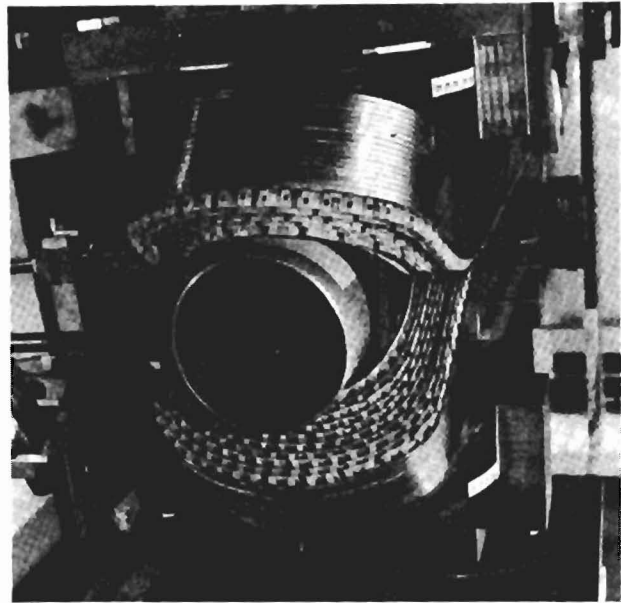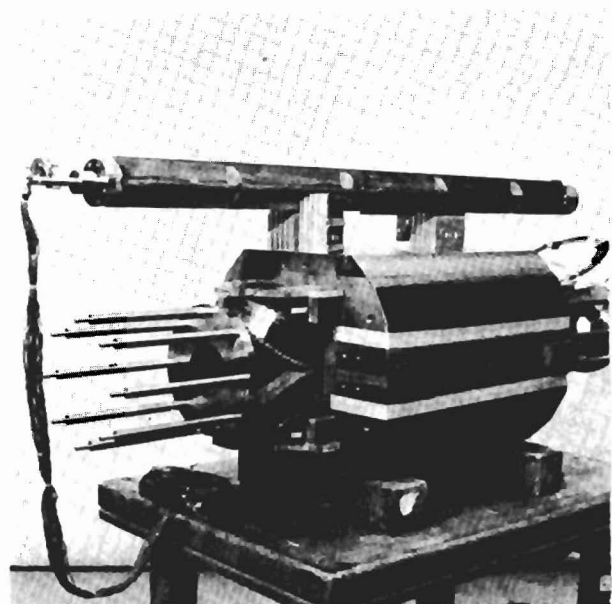Windings Inside.

Fig. 4.   Completed Assembly of 20-in. Model
Magnet with the Harmonic Search Coil
Probe Used for Field Measurements.

759

The 20-in. magnet was tested in a 2-ft diameter, 9-ft deep vertical dewar which was operated in closed circuit with a Model 1400 CTi helium refrigerator liquefier. Helium gas-cooled leads were used for both the dipole and sextupole coils with the gas being returned to the refrigerator. Fig. 5 shows the completed assembly of the model magnet with the top plate of the dewar before insertion in the dewar. It should be noted that in this test assembly, with the magnet supported from one end, the grooves in the aluminum cooling channel strips are horizontal rather than vertical as would be the case during normal operation as a beam magnet. Cooldown of the magnet and dewar to 4.5°K using the refrigerator required 22 hours.
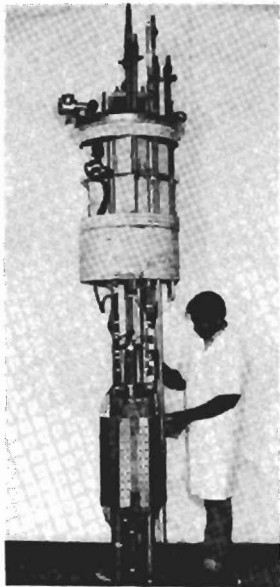

Fig. 5. Magnet Assembly Mounted on Dewar Top Plate Before Insertion in Dewar.

II. Field Measurement

The common magnetic field measurement technique involving the harmonic analysis of the integrated output of a search coil was used with the 20-in. model magnet. Very high sensitivities are attainable with this technique ($\pm$ 100 gauss-cm^2 for the product of the magnetic field and the effective area of the coil) so that accuracy is usually determined by electrical noise, mechanical errors in construction, alignment, or surveying of the coil device relative to the magnet coordinates. The harmonic search coil probe used for measurement of the 20-in. magnet, shown in

Fig. 4, contains an array of 2 long coils, 2 short coils, and 13 point coils. The long coils permit sampling of the integrated field through the magnet. Very high precision ($\sim 0.5 \times 10^{-4}$ parts) can be obtained with this technique by measuring differences between sampling coils and a coil in the probe designated as a reference coil.

Harmonic analyses were performed at a radius of 1.513 in. This corresponds to 80% of the radial position of the innermost super-conductor. The coefficients B_n of the multipole expansion of the field were obtained by measuring at 10° intervals:

$$B_r(r,\theta) = \sum_{n=1}^{\infty} B_n \left(\frac{r}{1.513}\right)^{n-1} \cos(n\theta + \alpha_n)$$

The preliminary results described in this paper were measurements giving the radial field components at 1.513 in. for both two-dimensional fields and the integral through the entire magnet. It should be noted that this data is taken at a larger radius than the radius of the semi-warm bore vacuum tube. The inner radius of the vacuum tube is 1.438 in., and the outer radius is 1.500 in. Only a minimal .188 in. is available for superinsulation to the 4°K surface with an inner radius of 1.688 in. The innermost super-conductor occurs at 1.875 in. radius. In general for warm bore applications, the beam tube will have to be as small as, or smaller than, this design. Thus particles will traverse the beam tube within a smaller radius than that at which the measurements were made with the harmonic coil. As far as the beam is concerned the amplitudes of higher harmonics will thus be much smaller.

Table II which is described next shows the radial scaling for all harmonics.

III. Two Dimensional Field Results

Table II lists the odd harmonics which are present in the internal or two dimensional part of the magnet. These are the terms which can be compared with the computed predictions, since only odd harmonics are permitted by symmetry for a "paper" magnet with 4 identical quadrants. The magnet has been cycled to above 40 kG. In all cases the measurements are made on a rising current cycle following a previous high field cycle. The field multipole amplitudes are normalized to the dipole amplitude. Positive and negative signs denote harmonics either in or out of phase respectively with the dipole at its poles.

Figure 6 shows the dipole field excitation versus current to 40 kG. The dipole field divided by the current, normalized to unity for infinite permeability is plotted. As can be seen, the magnet performs better than predicted by the computations, that is, saturation actually occurs $\sim$ 1 kG higher in field. This is principally due

TABLE II

Two Dimensional (Point Coil) Measurements at Radius =1.513-in. as a Function of Field

B_o(kG)	0.012	0.63	1.3	5.5	19.1	32.2	38.3[*]
I_{dipole}(A)	0.	15.35	30.4	132.1	463.8	851.5	1100.
$I_{sext.}$(A)	0.	0.	0.	4.0	7.6	145.7	240.
$3\theta/1\theta(r^2)$	-40.2%	-1.93%	-1.382%	+0.101%	-0.039%	+0.392%	+0.018%[†]
$5\theta/1\theta(r^4)$	-76.5	-0.67	-0.191	+0.077	+0.033	+0.065	+0.070
$7\theta/1\theta(r^6)$	- 7.5	+0.18	+0.236	+0.060	+0.025	-0.021	+0.023
$9\theta/1\theta(r^8)$	+ 6.5	+0.09	+0.010	-0.065	-0.041	-0.244	-0.306
$11\theta/1\theta(r^{10})$		+0.02	-0.044	-0.047	+0.015	-0.031	-0.033
$2\theta/1\theta$	+19.3	+0.40%		+0.069%	+0.041%	+0.042%	+0.144%
$4\theta/1\theta$	- 2.4	-0.05		-0.014	-0.004	+0.009	-0.014
$6\theta/1\theta$	- 2.8	-0.05		-0.011	-0.008	+0.009	-0.030
$8\theta/1\theta$	- 0.7	+0.04		+0.008	+0.003	+0.007	+0.028
$10\theta/1\theta$		+0.01		-0.001	-0.007	-0.016	

[*]Data taken at this field subject to more error; see text.

[†]The sextupole coefficients ($3\theta/1\theta$) can be made zero at all field levels and this change would have a negligible effect ($\leq 1 \times 10^{-4}$) on all other multipole coefficients.

to the fact that the low carbon steel used has a higher saturation field than obtained from the M-36 permeability curve used in the calculations. However, apart from the ~ 1 kG difference obtained in performance, the optical properties would not be significantly changed. For a fixed percentage dipole saturation which for the two types of steel would occur at slightly different absolute fields, the higher multipole aberrations will be identical to very high accuracy in these two cases. This is discussed further in a companion paper.[1]
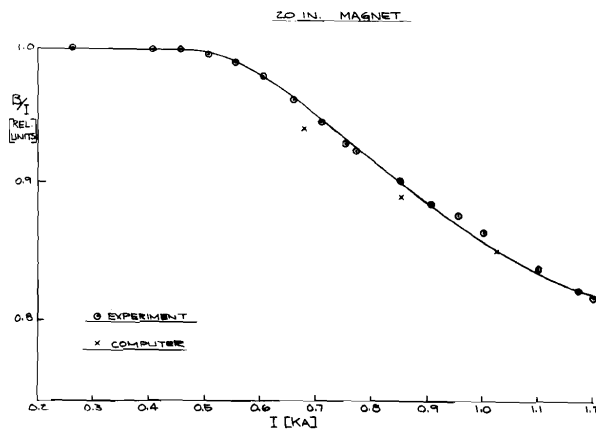
Fig. 6. Dipole Field B, Divided by Excitation Current I, as a Function of I to 40 kG.

We consider the results from 19 to 38 kG first because the lower field data are affected by infinite lifetime diamagnetic eddy currents in the superconductor. These must be superimposed on conventional magnetic circuit considerations.

At $\sim$ 19 kG (or below), a magnet of this type can be designed to have extremely uniform field over the entire aperture, without any sextupole correction required. The present 20-in. magnet, however, does have in its design, a small sextupole term. To correct for this term a very small correcting current is required whose amplitude is proportional to field even for large permeability.

From 19 to 38 kG, agreement between computation and the 20-in. model is good to 3×10^{-4} parts or better.[1] It must be stressed in looking at Table II that these are preliminary runs in which the sextupole coil has not been precisely set in current in each run. The 3θ term could be made identically zero with correct auxiliary coil settings. This auxiliary coil excitation is a simple function which is very accurately predictable by the computations after the permeability curve is accurately measured. Tuning out the small remaining sextupole has no significant effect on other harmonics. For example, the sextupole correction was set much less accurately for the 32 kG run than for the 18 or 38 kG runs. If the 32 kG run was repeated with 3θ identically zero, 5θ, 7θ and 11θ would change by less than 1×10^{-4} and 9θ would change by -2×10^{-4}. At 18 kG and 38 kG, no change would occur in any of the other terms by making 3θ identically zero.

Consider now the high field optical quality of this magnet. With sextupole removed, the dominant residual error is a 5θ term of $\sim 6 \times 10^{-4}$ parts. This agrees with the values computed in designing the model and could be made considerably smaller in later magnets. The large 9θ term is the first odd harmonic produced by the auxiliary sextupole coil. Its amplitude increases approximately linearly with field above saturation. At 40 kG it is $\sim 1 \times 10^{-4}$ parts at 1 in. radius, (55% of radial position of the innermost superconductor, r^8 radial dependance). This is more than adequate for the 8° magnet application. Moreover a more advanced design now exists which considerably reduces the 9θ term, with only a slight increase in mechanical complexity.

Let us now consider the additional effect of diamagnetism in the superconductors. The remanent field and the diamagnetic effects due to trapped flux in the sextupole coil have the fundamental symmetry of a 5θ term. (The 3θ term also contains some diamagnetism, as well as iron remanence.) The superconducting remanence vanishes by a few kilogauss, the diamagnetic effect then reverses sign and is of smaller amplitude.[2] This is apparent in the 5 kG data. This phenomenon will be studied further. However, the important point is that by 5 kG this magnet has quite small diamagnetic field errors. Comparing 5 kG to 19 kG (where the effects will be proportionately much smaller), it is apparent that the 5 kG diamagnetic contribution are already at the 3×10^{-4} parts level without any attempt at control or reduction.

Table II also lists the even harmonic terms measured, which give additional confirmation of the precision of the 20-in. magnet. Note that these results represent a direct measure of the ability to make a magnet as designed on paper; i.e., with no errors in construction or measurement, these even terms should all be zero.

The dominant even term at 19 and 32 kG is the lowest order term, the quadrupole 2θ. This is 4×10^{-4} parts at a radius of 1.513 in., or less than 3×10^{-4} parts per inch. This effect may be produced by a very small mechanical asymmetry.

As noted in Table II the 38 kG data were known to be subject to considerable error when taken because of electrical noise from the power supply. Such noise affects low multipoles most strongly, particularly quadrupole since it is strongest at four locations in the magnet. As a result the 2θ term at 38 kG is not considered real. The higher order error terms at 38 kG although small show considerably more experimental "noise" than the 18 and 32 kG results as well. The long coil measurements, discussed below, were subject to less noise and show smaller terms.

The higher order even terms from 5 kG to 32 kG are $\leq 1 \times 10^{-4}$ parts everywhere confirming the mechanical precision of the magnet. The +2.4 gauss quadrupole remanence is not fully understood, since it should not be allowed by symmetry to a very high degree of accuracy, as proven at higher fields yet it is $\sim$ 20% of the dipole. It is quite possible that this remanence is due to permanent magnetism in the 304 stainless steel of the inner tube and coil structure. The 8° magnets will use non-magnetic stainless steel. Consistent with this explanation is the fact that a constant +2.4 gauss scales exactly to +0.40% at 600 gauss.

If scaled to 5 kG and subtracted, the residual is $+3 \times 10^{-4}$ parts which in turn is very close to the $+4 \times 10^{-4}$ parts at 18 and 32 kG. Asymmetry in permanent magnetic structure in the stainless steel could indeed produce low order even multipoles.

IV. Magnet End Effects

The contributions of magnet ends to the odd harmonics are given in Table III. Listed are the amplitudes of the harmonics in the ends normalized by the integral dipole strength of the magnet. Note that for a 6-ft module of the 8° magnet, these terms will all be more than 3 times smaller than in this very short model. Even in the 20-in. model with 3θ up to $\sim 20 \times 10^{-4}$ parts, an impulse approximation in which the small end sextupole is averaged out internally would leave negligible optical error. Thus the auxiliary coil will ultimately be controlled for zero integral sextupole field.

Extrapolating to a 6-ft long module the remaining end effects will be very small with the exception of 5θ which will be $\sim -5 \times 10^{-4}$ parts. This might in some applications be excessive. However, this is a first try at end effect design. There are several parameters that can be varied to further reduce end effects if such refinement is required. If, for example, the ends have a constant term independent of saturation, adjustments of the "two-dimensional" magnet region can be made by computing small variations of the high permeability magnet to again make the integral aberration even smaller. This is an approach used at BNL for conventional magnets. These preliminary results for the 5θ term indeed show a constant value, at high fields which indicate that this technique is useful here. It is thus apparent that end effect design can easily be even further refined, since higher terms are already very small.

In Table III the even harmonics in the ends are given as well. The quadrupole term is relatively large, $\sim -10 \times 10^{-4}$ parts. This may be attributed in part to the stainless steel, as mentioned earlier. However, the dominant asymmetry is now probably due to the transposition of turns between layers at the end. Extrapolating to a 6-ft magnet this will be at the -3×10^{-4} level, which already compares favorably with conventional magnets. If this effect is verified in the 8° magnets, where it is not a problem, and when the non-magnetic stainless-steel center core will not contribute later magnets could have mechanical compensation built in.

The higher even harmonics are extremely small in the ends, indicating good control during construction.

TABLE III. End Effect (Integrating Coil-Point Coil) Measurements at Radius = 1.513-in. as a Function of Field.

B_o(kG)	19.1	32.2	38.3
I_{dipole}(A)	463.8	851.5	1100.
$I_{sext.}$(A)	7.6	145.7	240.
$3\theta/1\theta$	+0.222%	+0.035%	+0.172%
$5\theta/1\theta$	-0.155	-0.152	-0.174
$7\theta/1\theta$	-0.050	+0.065	+0.073
$9\theta/1\theta$	-0.010	+0.026	+0.039
$11\theta/1\theta$	+0.003	+0.002	+0.007
$2\theta/1\theta$	-0.090%	-0.087%	-0.128%
$4\theta/1\theta$	+0.020	+0.033	+0.027
$6\theta/1\theta$	+0.007	+0.012	-0.018
$8\theta/1\theta$	-0.004	-0.017	-0.018
$10\theta/1\theta$	-0.003	+0.001	-0.010

A final comment will be made on the 38 kG data. The long coil versus short coil, run, made to improve end effects (both coils at $\nu = 1.513$ in.) showed much less of a noise problem than the two dimensional run. As a result the 38 kG end effects are expected to be experimentally satisfactory. Indeed in Table III, the 38 kG run is well behaved in comparison with 32 kG and 19 kG. We feel that the higher terms in the short coil measurements described further above are spurious.

Finally, the integral harmonic contents of the model can be obtained by adding the same multipole entries in Tables II and III, keeping the signs as entered.

V. Magnet Performance

The initial tests have demonstrated the rugged nature of this magnet. It can be pulsed to its operating field for the 8° bend application (37 kG) in ~ 0.5 minutes. One can turn it off and let the current decay in seconds. This is a solid iron core magnet and such operations result in large losses. This fact has been demonstrated with a wattmeter. Nevertheless, the magnet does not go normal.

No training has been apparent. A field of 37 kG was attained on the first run, and by reducing power supply ripple a field slightly above 40 kG can be generated routinely. The magnet has been powered to date with large 120 volt SCR supplies used for conventional magnet testing. Conventional magnets of $> 10^5$ joules stored energy have been operated in series with the 20-in. magnet to provide more favorable load conditions for the supply. It is probable that these crude power supplies which have too much ripple by superconducting standards are limiting performance. When the maximum current at which the magnet is stable is exceeded, the dipole coil sometimes switches locally back and forth between the normal and superconducting state with a 60∿ and 360∿ modulation and the effect vanishes with a slight reduction in current. The 8° magnet will be operated with highly filtered low voltage supplies.

The only category in which the magnet is not totally up to expectations is the peak field. Small laminated Model No. 3[2] using these techniques goes essentially to short sample rating. It is probable that the noisy power supplies and the unlaminated solid core care playing a part in this. The short sample rating of the conductor at 40 kG and 4.2°K is twice the 40 kG magnet current and at 4.2°K the coil should be able to sustain 50 kG. However some parts of the coil experience higher local fields. In addition, the test cryostat is operating $\sim$ 0.5°K warmer than the temperature at which the short sample ratings were taken. Together these can reduce the margin by about one half. Of course the magnet operates well at the field of 37.5 kG which the 8° bending magnet application of the AGS calls for. Nevertheless the magnet should have reached $\geq$ 45 kG.

Attempting to understand this question, and get to expected performance is a major remaining question for projecting to large optimized systems, such as accelerators.

Questions about magnetic field quality, about magnet reproducibility, and about agreement with design computations have been largely resolved by this first prototype for the class of 40 kG window frame dipoles.

References

1. J.E. Allinger, et al., "Magnetic Circuit Considerations for High Field Magnets," these Proceedings.

2. G. Danby, et al., "Studies of Losses, Diamagnetic and Permanent Magnetic Effects in Superconducting Magnets," these Proceedings.